All in-fiber interferometric strain sensor based on cantilever Mach-Zehnder interferometer

HAIFENG ZHU[a,*], LIJUN LI[b,*], QIAN MA[b]
[a]*College of Science, China University of Petroleum, Shandong QingDao, 266580， China*
[b]*College of Electronic and Information Engineering, Shandong University of Science and Technology, Shandong Qingdao 266590, China*

A cantilever Mach-Zehnder interferometer (CMZI) strain sensor is proposed and its strain sensing characteristics are experimental demonstrated through investigating the dip wavelength and fringe visibility (FV) of its interference spectrum with the strain changing. While the strain increasing, the interference intensity dip wavelength appears blue shift, its FV shows increasing at the beginning, after achieves a maximin point, then decreases. At the range of its VF maximum, the wavelength versus strain presents the highest sensitivity. Therefore, using this CMZI sensor, high-sensitivity strain sensing can be obtained by controlling the sensing range near the maximum point of VF, and more large strain sensor range can be achieved by increasing the mismatching ratio of fiber cores. This device also can be applied to displacement, liquid level, refractive index and bending sensing.

(Received October 25, 2018; accepted June 14, 2019)

Keywords: Fiber optics sensor, Mach-Zehnder interferometer, Strain sensing, Cantilever

1. Introduction

In-line optical fiber interferometers, such as Mach-Zehnder interferometer [1], Michelson interferometers [2] and Fabry-Pérot interferometer [3], have received considerable attentions in recent years because of their all fiber compact structure, low cost, convenient operation and many sensing applications [4, 5]. Recently, optical fiber Mach-Zehnder interferometer (MZI) has attracted lots of interests in strain, micro-displacement and liquid level sensing. C. R. Liao et al. presented an in-line MZI strain sensor based on an air cavity fabricated by femtosecond laser at the single-mode fiber (SMF) core with 6.8pm/με sensitivity within 1800με [6]. Jiangtao Zhou et al. demonstrated a strain and temperature simultaneous measurement fiber in-line MZI based on misaligned a short section of thin core fiber (TCF) spliced between two sections of standard SMF [7]. Lecheng Li et al. proposed a singlemode-multimode-thinned-singlemode MZI sensor of axial strain measurement with sensitivity -2.99 pm/με and water level sensitivity -175.8 pm/mm, respectively [8]. Changyu Shen et al. proposed an optical fiber axial micro-displacement sensor based on MZI with sensitivity -0.385dB/μm, which was constructed by a bowknot-type taper combing with a fiber core-offset between two SMFs [9]. Bo Dong et al. reported a lateral force sensor based on a singlemode-multimode-singlemode optical fiber MZI [10]. Yuan Sun et al., fabricated a kind of strain sensor based on single mode-multimode-single mode optical fiber twisted MZI structure, in which different strain sensitivities were realized by controlling the torsional number of the circles of the sensing fiber [11]. Adel Abdallah, proposed a novel strain sensor based on a hollow-core photonic bandgap fiber MZI interferometric structure [12]. Fan Yang et al. demonstrated an MZI strain sensor based on a multimode fiber- photonic crystal fiber cascaded structure with -14.89pm/με sensitivity [13]. However, some abovementioned optical fiber in-line MZIs is fabricated by using relatively complex and high-cost method and devices. Moreover, in all above MZI sensors, the strain is directly loaded onto the bare optical fiber, which will make the sensor easy to be broken and difficult to achieve practical application.

In this paper, a kind of CMZI (cantilever in-line Mach-Zehnder interferometer) strain sensor is fabricated by pasted a single mode-mulitmode-thin core-multimode-single mode optical fiber MZI on a metal cantilever. In this sensor, strain is applied on the cantilever end rather than directly on the bare optical fiber, thus the strain rupture can be avoided. In our experiments, the strain versus interference dip wavelength and its fringe visibilities (FV) intensity of CMZI interference relationship curves are gotten, which shows that the dip wavelength has blueshift within 0-636με, and the fringe visibilities (FV) intensity presents gradually increase at the beginning, and decrease after gets the maximum value, meanwhile, near the VF maximum point, the wavelength versus strain can get the highest sensitivity.

2. Theory

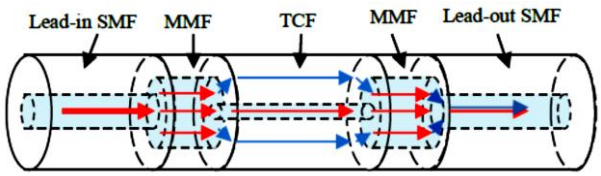

Fig.1. The schematic diagram of the in-line MZI

In our experiments, the schematic of the MZI is shown in Fig. 1. A 15mm long TCF is spliced between two 5mm long step index multimode optical fibers (MMFs), the core/cladding diameter of MMF is 105/125μm. These sections are spliced between two standards SMF. The TCF has mode field diameter of 4.5μm at 1550nm wavelength and 125μm cladding diameter, respectively. Through the first lead-in SMF, the light is launched into the first MMF as shown in Fig. 1. At its first splice point, the light power is divided into two parts. One part still transmits in the fiber core, another part of the light power can be coupled to the cladding and multi-cladding modes can be excited because of large diameter mismatch between SMF and MMF1. Similarly, at the first splicing point between MMF and TCF, the light power is also split into two portions due to the mode field mismatch. At the TCF-MMF splice point, part of the TCF cladding modes that couple back into the core of the MMF. Consequently, they are recoupled into the core of lead-out SMF and interferent. The interference spectrum is formed by cladding and core modes and its transmission spectrum can be expressed as [14]

$$I_{out} = \left(E_0\gamma\beta\right)^2 + \left[E_0\left(1-\gamma\right)\right]^2 + 2E_0^{\,2}\gamma\left(1\text{-}\gamma\right)\beta\cos\left(\frac{2\pi\Delta n_{eff}}{\lambda}\right) \quad (1)$$

where, E_0 is the electrical field amplitude of launched field into the fiber. γ is the splitting ratio between core and cladding light power in the TCF, β is the propagation loss of cladding mode, n_{eff} is the difference of the effective refractive indices between core and cladding modes, L is the geometry length of the TCF, and λ is the wavelength of the propagating light.

The interference dip wavelength of this MZI spectrum can be written as [15]

$$\lambda_m = 2\Delta n_{eff} L/\left(2m+1\right) \quad (2)$$

where, m is an integer, which means the number of cladding modes. The fringe visibility of the MZI spectrum can be expressed as

$$V = 2\beta\left(\beta^2\frac{\gamma}{1-\gamma}+\frac{1-\gamma}{\gamma}\right) \quad (3)$$

where, V is fringe visibility.

This MZI is pasted on a cantilever, which structure is shown in Fig. 2. If a load P is applied at the free end of the cantilever, the cantilever will bend with it, and the tensile strain will be caused on the beam surface. The bending moment M of section x_0 on the cantilever can be express as [15]

$$M = \left(d-x_0\right)P \quad (4)$$

where, d is the length of this cantilever. x_0 is the TCF pasted section. The stress δ along beam axial direction is

$$\delta = Mh/2I = \left(d-x_0\right)Ph/2I \quad (5)$$

where, h is the thick of the cantilever. I is inertia moment of x_0 section.

The strain ε_x of the cantilever caused by load P can be approximated as

$$\varepsilon_x = \delta/E = \left(d-x_0\right)Ph/2EI \quad (6)$$

where, E is elasticity modulus of the spring steel material of the cantilever.

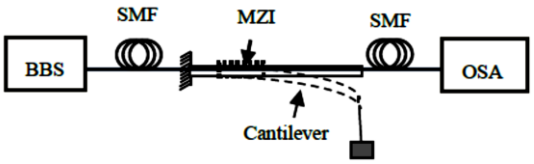

Fig. 2. Spring steel cantilever and experimental setup

3. Experimental results and discussions

In order to get more sensitive to the strain, the sensing part TCF of the MZI is pasted on the center and nearly closed to the fixed end of the cantilever. In our experiment, the length, thick, width and TCF stick section of the cantilever is 100mm, 0.5mm, 15mm and 30mm, respectively. Experimental setup is shown in Fig. 2. A broadband optical source (BBS) is used to inject light into the MZI, and an optical spectrum analyzer (YOKOGAWA AQ6370) is used to measure the spectral response of the senor. In order to eliminate the disturbance of the light source, a subtract between the measured spectrum of the sensor and the original spectrum of the light source was done.

Fig. 3 shows the overlap of transmission interference spectrum of the strain increasing step by step from 0 to

636με at the room temperature (20℃). From this figure, it can be found that there are three obvious interference transmission dips. These dip wavelengths and their fringe visibilities are gradually shift with the strain increase. Two curves of the relationship between the dip wavelength and its fringe visibility versus the strain are shown in Fig. 4. We can find that the dip wavelength shows a blue shift with strain and its fringe visibility shows increase at the beginning of the strain increasing, after gets a maximum point, then it shows decrease with the strain increase. The observed wavelength in Fig. 4 and its drift trend are marked by arrows. Other dips can also be used as observation wavelength, because they come from different cladding modes, and all of them have different strain sensitivities. From the sensing principle, we can know that their temperature variation is the same, so, other wavelength measurements can be used to eliminate the temperature cross-sensitivity of this type of strain sensor.

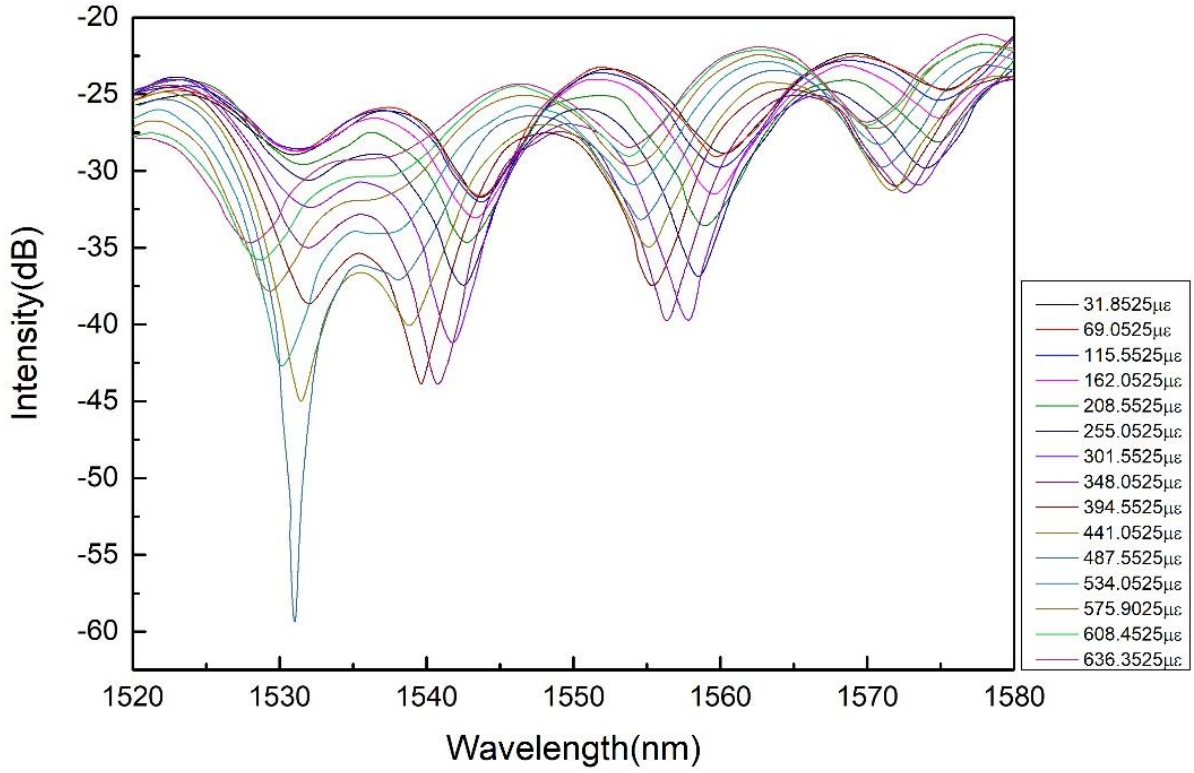

Fig. 3. The overlap spectra of the CMZI through loading

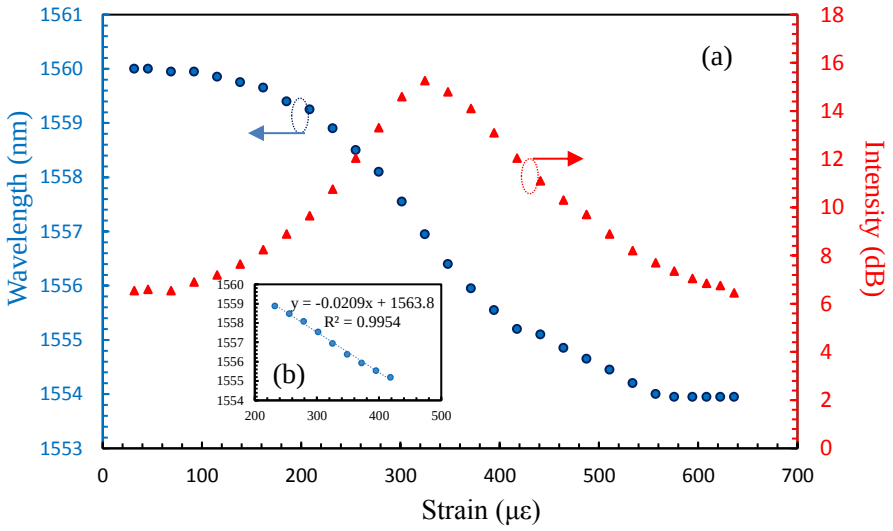

Fig. 4. (a) Dip wavelength and its fringe visibilities change with strain curves and (b) linearly fitting curve of experiment data near the VF maximum point

It can be analyzed as follows: at the beginning, the interference dip wavelengths changed smoothly with the strain increasing on the cantilever, because the stress is relatively small and resulting in cantilever bending is not enough, the wavelengths change mainly caused by the core-cladding offset [4]. With the strain continue increase, the wavelength drifts appear higher sensitivity than that of before, which is due to that at that time, the wavelengths shift is caused by the combination of core-cladding offset and the interference length being stretched. From Fig. 4, it can be observed that, with the strain increasing, the FV began to grow gradually, after the relatively FV reached the maximum value, the FV begin to gradually decreases with the increase of the strain. This can be explained by Eq. (3). According to MZI, the FV in the interference pattern depends strongly on the ratio of lights coupled into the core and cladding in TCF. In this sensor, the TCF is the mainly sensitive part. The bending of the TCF can cause the change of the coupling coefficient (γ). Therefore, as the coupling coefficient increases gradually approaching the optimum coupling point (the point that transmission depth reached the maximum value) corresponding to the two sections of the end face of an optical fiber coupling coefficient. With the strain continue increase, the cantilever continues to bend, the fiber coupling position continues to change, and the coupling coefficient is also changed. At this time, the transmission depth is gradually reduced. By comparing two curves in Fig. 4, it can be seen that the wavelength versus strain sensitivity is high near the maximum VF point, which can get -20.9pm/με.

4. Conclusions

In conclusion, a CMZI device is proposed and its strain sensing characteristics are experimental studied. As we known, the interference spectrum of this kind of in-line MZI are come from the interference between core modes and several low-order cladding modes [2]. In this experiment, several interference dip wavelengths are existing in the CMZI spectrum. The interference dip wavelengths have same strain performance. The dip wavelengths all appearance blue shift with the strain increasing. At the beginning, wavelength shift with strain increase shows small sensitivity. As the strain continues to be increased, the sensitivity of the sensor is significantly improved. The relationship between fringe visibility and strain of the interference dip wavelengths are also studied. With the strain raised, FV is begun to grow gradually, after reachig the maximum point, the FV begin to decrease. The highest wavelength versus strain sensitivity exists at the range of near the maximum point with -20.9pm/με. From this experiment, using this CMZI strain sensor, high-sensitivity measurement can be obtained by controlling the sensing range near the maximum point of VF, and the strain sensor range can be expanded by increasing the mismatching ratio of fiber cores, in order to meet the requirements of different strain sensing.

Acknowledgements

This work is supported by the Shandong Provincial Natural Science Foundation of China (No. ZR2009AM017 and No.ZR2013FM019), the National Postdoctoral Project of China (No. 200902574 and 20080441150), Shandong Provincial Education Department Foundation of China (No.J06P14).

References

[1] Lecheng Li, Li Xia, Zhenhai Xie, Deming Liu, Opt. Express **20**, 11109 (2012).
[2] Tingting Wang, Ming Wang, IEEE Photonics Technology Letters **24**, 1733 (2012).
[3] Lijun Li, Qian Ma, Maoyong Cao, Guina Zhang, Yan Zhang, Lu Jiang, Chunting Gao, Jia Yao, Shun Shun Gong, Wenxian Li, Sensors and Actuators B: Chemical **234**, 674 (2016).
[4] Linh Viet Nguyen, Dusun Hwang, Sucbei Moon, Dae Seung Moon, Youngjoo Chung, Opt. Express **16**, 11369 (2008).
[5] Lijun Li, Qian Ma, Yan Zhang, Maoyong Cao, Guina Zhang, Lu Jiang, Chunting Gao, Jia Yao, Yidan Li, Shunshun Gong, Wenxian Li, Sensors and Materials **29**, 15 (2017).
[6] C. R. Liao, D. N. Wand, Ying Wang, Opt. Lett. **38**, 757 (2013).
[7] Jiangtao Zhou, Changrui Liao, Yiping Wang, Guoyu Yin, Xiaoyong Zhong, Kaiming Yang, Bing Sun, Guanjun Wang, Zhengyong Li, Opt. Express **22**, 1680 (2014).
[8] Changyu Shen, Youqing Wang, Jinlei Chu, Yanfang Lu, Yi Li, and Xinyong Dong, Opt. Express **22**, 31984(2014).
[9] Bo Dong, Da-Peng Zhou, Li Wei, Wing-Ki Liu, John W. Y. Lit, Opt. Express **23**, 19291 (2008).
[10] Jiangtao Zhou, Yiping Wang, Changrui Liao, Bing Sun, Jun He, Guolu Yin, Shen Liu, Zhengyong Li, Guanjun Wang, Xiaoyong Zhong, Jing Zhao, Sensor and Actuators B **208**, 315 (2015).
[11] Yuan sun, Deming Liu, Ping Lu, Qizhen Sun, Wei Yang, Shun Wang, Li Liu, Wenjun Ni, Optics Communications **405**, 416 (2017).
[12] Adel Abdallah, Optics Communications, **428**, 35 (2018).
[13] Fan Yang, Z. K. Wang, D. N. Wang, Optical Fiber Technology **47**, 102 (2019).
[14] Jun Su, Zhengrong Tong, Ye Cao, Weihua Zhang, Optics Communications **315**, 112 (2014).
[15] Li Lijun, Zhang Xu, Tang Bin, Shi Jing, Yuan Xuemei, Lai Yongzheng, Li Jing, Sui Tao, Zhang Yanliang, Cao Maoyong, Journal of China Coal Society **38**(11), 2094 (2013).

*Corresponding author: nankaillj@163.com;
zhufeng_97@upc.edu.cn